

# Performance Analysis of a Prototype High-Concentration Photovoltaic System Coupled to Silica Optical Fibers

Giuseppe Mattia Lo Piccolo,\* Adriana Morana, Aziz Boukenter, Sylvain Girard, Youcef Ouerdane, Fabio Maria Montagnino, Franco Mario Gelardi, Simonpietro Agnello,\* and Marco Cannas

High-concentration photovoltaic (HCPV) systems are one of the most promising technologies for the generation of renewable energy with high-conversion efficiency. Their development is still at an early stage, but the possibility of integrating high-concentration systems into buildings offers new opportunities to achieve the net-zero-energy building goal. Herein, the optical and energetic performance of a hybrid daylighting–HCPV prototype based on pure- or doped-silica optical fibers (OFs) to guide  $2000\times$  concentrated sunlight inside the buildings is evaluated. There, the light can either be used to illuminate interior spaces or projected on solar cells to generate electricity. The system equipped with a single  $400\ \mu\text{m}$  core-diameter OF is demonstrated to achieve a total efficiency of 15% and an optical efficiency of 45%.

modules, and for this reason HCPV stations today remain mostly limited to large-scale solar plants.<sup>[5]</sup> To increase their functionality and accessibility, new-generation HCPV devices should have simpler architectures, lower cost, and should use commercially available parts for an easier and cheaper manufacturing. This would open new market segments and would give a strong impulse to the integration of HCPV in commercial and residential buildings.

As demonstrated by Núñez et al.,<sup>[6,7]</sup> CPV and daylighting (DL) technologies share the same needs in terms of infrastructures and are compatible to be integrated into the same module. Although


many DL and hybrid DL/CPV modules have been proposed in the past ten years,<sup>[7–14]</sup> none of them have reached the commercial stage yet. The idea behind most of these devices is to use a tracking solar concentrator coupled to optical fibers (OFs) to harvest the sunlight and guide it inside a building. The transmitted light can then be used to directly illuminate any interior living spaces or redirected to an array of solar cells for electricity generation. Although promising, this idea has not yet been fully developed and the efficiency of the proposed hybrid modules remains still too low to meet the energy and illumination demand of buildings.<sup>[15]</sup> For this reason, new concepts are

## 1. Introduction

In recent years, solar energy has attracted the attention of scientists and investors around the world as an alternative source of renewable energy with low environmental impacts. Thanks to the high energy yield per square meter, high productivity throughout the day, and the reduction of material costs, high-concentration photovoltaic (HCPVs) systems are now assuming a predominant role in the solar energy market.<sup>[1–4]</sup> However, the complex design and the need for sophisticated tracking systems account for larger space requirements as compared with traditional PV

G. M. Lo Piccolo, Prof. F. M. Gelardi, Prof. S. Agnello, Prof. M. Cannas  
Dipartimento di Fisica e Chimica – Emilio Segrè  
Università degli Studi di Palermo  
Via Archirafi 36, 90123 Palermo, Italy  
E-mail: giuseppemattia.lopiccolo@unipa.it;  
simonpietro.agnello@unipa.it

G. M. Lo Piccolo  
Dipartimento di Fisica e Astronomia “Ettore Majorana”  
Università degli Studi di Catania  
Via Santa Sofia 64, 95123 Catania, Italy

 The ORCID identification number(s) for the author(s) of this article can be found under <https://doi.org/10.1002/pssa.202100027>.

© 2021 The Authors. physica status solidi (a) applications and materials science published by Wiley-VCH GmbH. This is an open access article under the terms of the Creative Commons Attribution License, which permits use, distribution and reproduction in any medium, provided the original work is properly cited.

DOI: 10.1002/pssa.202100027

Dr. A. Morana, Prof. A. Boukenter, Prof. S. Girard, Prof. Y. Ouerdane  
UJM-Saint-Etienne  
CNRS  
IOGS  
Lab. Hubert Curien UMR 5516  
Univ-Lyon  
18 Rue Pr. B. Luras, 42000 Saint-Etienne, France

F. M. Montagnino  
The Cyprus Institute  
20 Konstantinou Kavafi Street, 2121 Aglantzia, Nicosia, Cyprus

F. M. Montagnino  
IDEA s.r.l.  
C.da Molara Z.I. III Fase  
90018 Termini Imerese, PA, Italy

Prof. S. Agnello  
ATeN Center  
Università degli Studi di Palermo  
Viale delle Scienze Ed. 18, 90128 Palermo, Italy

needed to achieve higher efficiencies and contribute to reducing the environmental impact of buildings.

The objective of this study is to test the stability of different commercial OFs to concentrated sunlight and evaluate the efficiency of a prototypical fiber-based DL/HCPV module. In our previous work we demonstrated that Al- and P-doped silica fibers show a significant signal loss due to the photoinduced formation of point defects (solarization), whereas pure silica, Ge-doped silica, and F-doped silica fibers have good resistance to the broadband light produced by a laser-driven light source.<sup>[16]</sup> For this reason we decided to field test the latter fibers by mounting them on our recently developed hybrid module and study their transmission properties as a function of exposure time. This is the first study exploring the effects of 2000× concentrated sunlight on commercial OFs of different chemical compositions. The experimental results allowed us to verify the absence of ongoing solarization processes in the selected OFs and identify the most suitable waveguides for solar energy applications. This information will guide us to further improve the performance of our hybrid DL/HCPV module and improve its design for its future release in the building-integrated photovoltaic market.

## 2. Results and Discussion

The transmission properties of the fibers shown in **Table 1** were studied by measuring the power generated by a triple-junction (TJ) solar cell coupled to each of them, as explained in **Section 4**. To allow a direct comparison between the various fibers, the power output of each cell ( $P_{\text{cell}}$ ) was normalized to the direct normal irradiance (DNI) using the formula

$$P_n = \frac{P_{\text{cell}}}{\text{DNI}} \quad (1)$$

where  $n$  is the fiber label. The results shown in **Figure 1** indicate that the mean normalized power outputs of the cells coupled to the chosen fibers are as follows:  $\bar{P}_{\text{FP200ERT}} = 4.5 \pm 0.1$  mW,  $\bar{P}_{\text{FP200URT}} = 2.0 \pm 0.1$  mW,  $\bar{P}_{\text{FP400ERT}} = 20 \pm 1$  mW,  $\bar{P}_{\text{GeMM}} = 0.10 \pm 0.03$  mW, and  $\bar{P}_{\text{IXF-CUST-SiO}_2/\text{F}} = 0.4 \pm 0.1$  mW. The uncertainty characterizing the data is, in general, correlated with the sample cleavage quality, the alignment with the mirror optical axis, and the accuracy of the tracking system. In the case of FP400ERT, the error is most likely due to the suboptimal weather

**Table 1.** Technical specifications for the tested OFs. HP stands for hard polymer.

Label	Manufacturer	Core/cladding material	Core diameter [μm]	Transmission range [nm]	NA
FP200ERT	Thorlabs	Low-OH SiO <sub>2</sub> /HP	200	400–2200	0.50
FP200URT	Thorlabs	High-OH SiO <sub>2</sub> /HP	200	300–1200	0.50
FP400ERT	Thorlabs	Low-OH SiO <sub>2</sub> /HP	400	400–2200	0.50
GeMM	Thorlabs	SiO <sub>2</sub> :GeO <sub>2</sub> /SiO <sub>2</sub>	62.5	400–2200	n.d.
IXF-CUST-SiO <sub>2</sub> /F	Thorlabs	SiO <sub>2</sub> /SiO <sub>2</sub> :SiF	62.5	400–2200	0.12

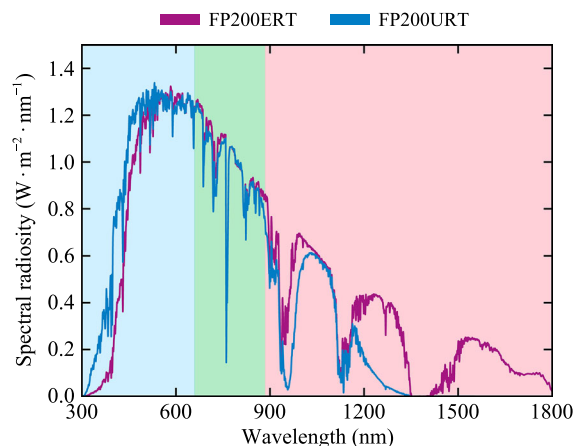


**Figure 1.** Solar spectral irradiance as transmitted by the fibres FP200ERT (low-OH) and FP200URT (high-OH). The fibre FP400ERT, being a low-OH, has the same spectral irradiance as FP200ERT. The shaded areas correspond to the spectral response range of the InGaP (300–660 nm), InGaAs (660–885 nm), and Ge (885–1850 nm) subcells of a triple-junction solar cell.

conditions on the day of the measurements. In fact, due to the shadow cast by the moving cloud, the variation of the instantaneous DNI was estimated to be ≈15% and this was partially reflected on the uncertainty characterizing the  $\bar{P}_{\text{FP400ERT}}$  data. In spite of this, the ratio  $\bar{P}_{\text{FP400ERT}}/\bar{P}_{\text{FP200ERT}}$  is approximately equal to 4, confirming the expectations given by the cross-sectional areas of the two fibers. The difference between  $\bar{P}_{\text{FP200URT}}$  and  $\bar{P}_{\text{FP200ERT}}$ , in contrast, may be attributed to the different chemical compositions of the two OFs. In fact, despite both being pure-silica core fibers, FP200ERT is characterized by a low concentration of hydroxyl (OH) groups, whereas FP200URT has a higher concentration of them. This difference is very important for the transmission properties of the fibers as it determines their signal transmission efficiency in the ultraviolet (UV) and near-infrared (NIR) spectral regions.<sup>[17,18]</sup>

In general, the OH groups bonded to the glass network of silica fibers have fundamental stretching vibrations between 2700 and 4200 nm, depending on the position of the group. These fundamental vibrations give rise to multiple-overtone bands located at 1380, 950, and 720 nm and combination bands at 1240, 1130, and 880 nm.<sup>[19]</sup> This means that high-OH OFs are not able to transmit light of wavelength longer than 1200 nm and are better used for UV–vis light applications. In contrast, low-OH OFs have low attenuation throughout the vis–NIR spectral range but fail at guiding UV light.<sup>[20]</sup> To investigate the influence of fiber attenuation on the intensity of the photogenerated current, we calculated the spectral radiosity transmitted by FP200ERT and FP200URT as

$$J(\lambda) = E_0(\lambda)e^{-A(\lambda)L} \quad (2)$$

where  $L$  is the sample length (2.50 m in both cases),  $E_0(\lambda)$  is the direct solar irradiance AM1.5D,<sup>[21]</sup> and  $A(\lambda)$  is the fiber spectral attenuation declared by the manufacturer.<sup>[22]</sup> The curves in **Figure 2** show that low-OH fibers transmit sunlight better than high-OH ones and that the biggest difference is in the NIR

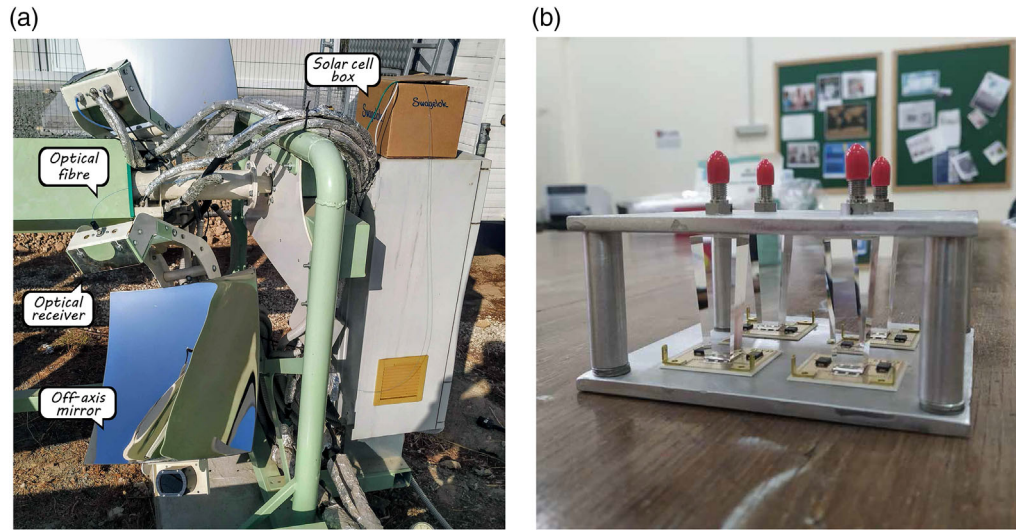


**Figure 2.** Pictures of the real DL/HCPV module showing a) the architecture of the device and b) an array of solar cells used during the tests.

domain. FP200URT has a high transparency in the 300–1200 nm range but blocks longer wavelengths, whereas FP200ERT works better in the 400–2200 nm range but has significant loss in the UV domain. As the intensity of the current produced by the TJ cells is limited by the subcell receiving the lowest amount of light,<sup>[23]</sup> the  $\bar{P}$  values observed for the two fibers depend on both the radiant flux and the spectral distribution of the transmitted sunlight. By integrating  $J(\lambda)$  and  $E_0(\lambda)$  over the spectral response range ( $\Lambda$ ) of the three subcells, we can determine the theoretical percent transmittance of the fibers as

$$T = \frac{\int_{\Lambda} J(\lambda) d\lambda}{\int_{\Lambda} E_0(\lambda) d\lambda} \quad (3)$$

where  $\Lambda_1 = [300 \text{ nm}, 660 \text{ nm}]$  for the InGaP layer,  $\Lambda_2 = [660 \text{ nm}, 885 \text{ nm}]$  for the InGaAs layer, and  $\Lambda_3 = [885 \text{ nm}, 1850 \text{ nm}]$  for the Ge layer. The results shown in **Table 2** reveal that the lowest transmittance for FP200ERT fiber is in the range  $\Lambda_2$ , whereas that for FP200URT fiber is in the range  $\Lambda_3$ . This implies that the efficiency of the solar cell coupled to these fibers is limited by the current generated by, respectively, the InGaAs and the Ge subcells. The ratio between the two limiting transmittance values ( $29\%/52\% = 0.56$ ) is compatible with the ratio  $\bar{P}_{\text{FP200URT}}/\bar{P}_{\text{FP200ERT}} = 0.4 \pm 0.2$ , confirming that the difference observed for the two time series is largely determined by the intrinsic absorption spectrum of silica.

**Table 2.** Percent transmittance of the fibers FP200ERT and FP200URT in the spectral response range ( $\Lambda$ ) of the InGaP (300–660 nm), InGaAs (660–885 nm), and Ge (885–1850 nm) subcells of a TJ solar cell.

$\Lambda$ [nm]	$T_{\text{FP200ERT}}$	$T_{\text{FP200URT}}$
300–660	71%	88%
600–885	52%	51%
885–1850	56%	29%

Due to the small diameter and low numerical aperture (NA), only a modest amount of light was injected into the GeMM and IXF-CUST-SiO<sub>2</sub>/F samples. The photocurrent produced by the relative solar cells ( $\approx 20 \mu\text{A}$ ) is comparable with the noise current and for this reason the values of  $\bar{P}_{\text{GeMM}}$  and  $\bar{P}_{\text{IXF-CUST-SiO}_2/\text{F}}$  are close to zero. For the F-doped sample, this behavior is uniquely determined by the size of the fiber, as demonstrated by the following relation:

$$\frac{r_{\text{IXF-CUST-SiO}_2/\text{F}}^2}{r_{\text{FP200ERT}}^2} \approx \frac{\bar{P}_{\text{IXF-CUST-SiO}_2/\text{F}}}{\bar{P}_{\text{FP200ERT}}} \approx \frac{1}{10} \quad (4)$$

where  $r$  is the fiber core radius. The case of GeMM, on the contrary, is more complicated as the cross-sectional area ratio (with respect to FP200ERT) is equal to 1/10, whereas the  $\bar{P}$  ratio is 1/45. This suggests that the low power output measured for this sample is not only determined by the small fiber diameter but is also due to a higher attenuation of the transmitted light. In fact, Ge-doped fibers are generally used for telecommunication applications and their composition is optimized to achieve the highest transparency in the IR wavelength range. Although their theoretical transmission range extends from 400 to 2000 nm, the attenuation level in the visible domain is generally higher than that of pure silica and for this reason the radiant flux transmitted by the fiber is much lower than that measured for FP200ERT.

To further validate the results, we conducted a second test consisting of the simultaneous exposure of all fibers to concentrated sunlight. For this test, four additional HCPV modules were upgraded to host the fibers, and each of them was coupled to a different TJ cell. As observed in the previous case, the time series shown in **Figure 3** is constant over time and the corresponding mean normalized power is  $\bar{P}_{\text{FP200ERT}} = 4.7 \pm 0.2 \text{ mW}$ ,  $\bar{P}_{\text{FP200URT}} = 2.2 \pm 0.1 \text{ mW}$ ,  $\bar{P}_{\text{FP400ERT}} = 19.8 \pm 0.9 \text{ mW}$ ,  $\bar{P}_{\text{GeMM}} = 0.11 \pm 0.03 \text{ mW}$ , and  $\bar{P}_{\text{IXF-CUST-SiO}_2/\text{F}} = 0.3 \pm 0.2 \text{ mW}$ . These values are compatible with those shown in Figure 1 and for this reason we can affirm that the outcomes of the day-long, single-fiber

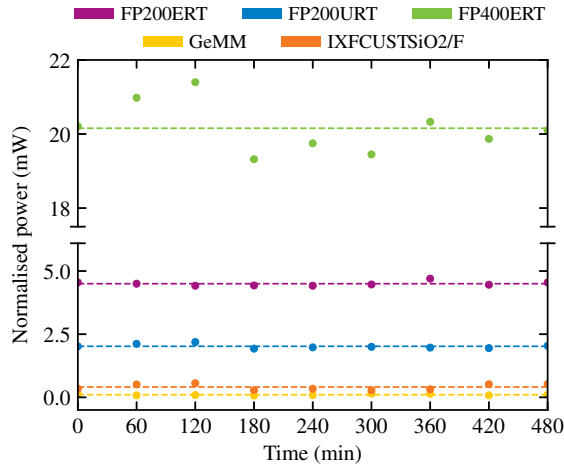


**Figure 3.** Time series plot of the normalized power measured for the tested samples during the 8 h exposure to concentrated sunlight. The dashed lines indicate the mean normalized power for each data set.

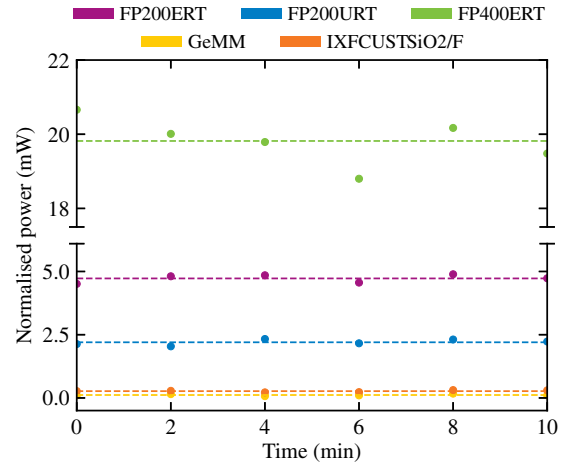


**Figure 4.** Time series plot of the normalized power measured for the tested samples during the 10-min exposure to concentrated sunlight. The dashed lines indicate the mean normalized power for each data set.

tests are reliable and are equivalent to the results we would have obtained by testing all the fibers at the same time.

The total power efficiency of our hybrid system can be calculated as

$$\eta_T = \frac{P_{\text{out}}}{P_{\text{in}}} \quad (5)$$

where  $P_{\text{out}}$  is the maximum normalized power generated by the cell and  $P_{\text{in}}$  is the radiant flux injected into the fiber (i.e., the DNI). As our aim is to calculate the maximum efficiency of the system, in the following calculation, we will refer to FP400ERT which is the sample with the highest  $\bar{P}$ . To be transmitted, the light hitting the entry face of the sample must form an angle with the optical axis lower than or equal to the acceptance angle  $\theta$  of the fiber. Considering that FP400ERT has an NA of 0.50, the injection condition is

$$\theta = \sin^{-1}(\text{NA}) = 30^\circ \quad (6)$$

and the portion of the mirror surface effectively coupled to the fiber is

$$A_M = \pi(\text{EFL} \cdot \tan \theta)^2 = 1380 \text{ cm}^2 \quad (7)$$

with EFL being the mirror effective focal length (36.3 cm). This corresponds to the area of the circle being formed by the intersection of the mirror with the light cone subtended by the OF (the dark-blue beam in **Figure 4**). Knowing that the maximum solar irradiance measured during the test of FP400ERT is  $E_{\text{Sun}} = 768 \text{ W} \cdot \text{m}^{-2}$ , we can calculate the maximum radiant flux injected into the fiber as

$$\Phi_M = E_{\text{Sun}} A_M = 106 \text{ W} \quad (8)$$

As the mirror focal image has an area ( $A_{\text{MFI}}$ ) of  $1 \text{ cm}^2$  and the cross-sectional area of FP400ERT is  $A_F = 1.26 \times 10^{-3} \text{ cm}^2$ , the flux collected by the fiber is

$$\Phi_F = \frac{\Phi_M A_F}{A_{\text{MFI}}} = 134 \text{ mW} \quad (9)$$

By taking  $\Phi_F$  as the radiant flux injected into the fiber and  $\bar{P}_{\text{FP400ERT}}$  as the maximum normalized power generated by the cell, the total power efficiency of the system results in

$$\eta_T = \frac{P_{\text{out}}}{P_{\text{in}}} = \frac{\bar{P}_{\text{FP400ERT}}}{\Phi_F} = 0.15 \quad (10)$$

This value is useful to estimate the system's ability to produce electricity from sunlight but provides little information on the quality of the optical coupling between the mirror and the fiber. This information can be obtained by considering that, for our system

$$\eta_T = \eta_o \eta_e \quad (11)$$

where the first factor is the optical efficiency of the mirror–fiber coupling and the second is the electric conversion efficiency of the cell. As we know that  $\eta_e = 0.33$ ,<sup>[24]</sup> the optical efficiency of the system can thus be calculated as

$$\eta_o = \frac{\eta_T}{\eta_e} = 0.45 \quad (12)$$

This result clearly proves that 1) the DL/HCPV module is able to guide sunlight to a remote array of solar cells placed in a controlled environment and that 2) the OFs resist to a full day of highly concentrated sunlight without losing their transparency in the range of interest. The latter aspect is of particular importance as it suggests that the silica matrix of the OFs is not damaged by solar radiation and that the efficiency of the defect formation processes is close or equal to zero. This means that a prolonged fiber exposure would not lead to a significant attenuation level as dose-dependent effects are unlikely at the energies of the solar spectrum. Further surveys should, however, be conducted on this

topic to confirm our model and understand the implications of fiber aging on the performance of hybrid solar devices.

To increase the performance of the system, the first issue to be addressed is the thickness of the chosen OFs. Bigger fibers would deliver more sunlight to the cells but would also increase the cost and the mechanical constraints of the system. As an alternative, we could opt for an OF bundle, i.e., a cable composed of many fibers put together, to increase the collecting surface exposed to the sunlight. The main advantage of a bundle is that its size can be controlled to match the size of the image formed at the mirror focus. In either case, a trade-off between compactness and efficiency is necessary to develop a market-ready technology. The second issue is the coupling between the mirror and the OF(s). This could be partially solved using a secondary optical element such as a fiber end cap or a reverse-beam expander. However, as light is reflected and scattered at each air–glass interface, a higher number of elements in the optical path means a higher light loss and hence a lower overall efficiency. In our future investigations, we will explore the possibility of integrating the HCPV system with either bundles or fibers of larger diameter. We will also determine the conversion efficiency in each case and conduct a cost-to-benefit analysis to estimate the strengths and weaknesses of the various alternatives.

### 3. Conclusion

We have analyzed the optical and energy production performance of a prototypical photovoltaic device able to transport sunlight into building interiors for either natural illumination or electricity production through TJ solar cells. The proposed daylighting HCPV (DL/HCPV) module makes use of off-axis parabolic mirrors to collect the sunlight and focus it on OFs with a  $2000\times$  concentration ratio. It has been verified that the highest transmission efficiency is achieved by using 0.50 NA OFs made of high-purity, low-hydroxyl vitreous silica with a core diameter of  $400\mu\text{m}$ . We have also verified that no degradation of the fiber transmission occurs under  $2000\times$  concentrated sunlight. The total and optical efficiency of the system is, respectively, 15% and 45%, which represents a good result given that the mirror was coupled with just one bare OF.

### 4. Experimental Section

**The HCPV System:** The HCPV system used as a basis to build the hybrid module was developed by IDEA Srl and is currently installed at the “Università degli Studi di Palermo,” Italy. It was composed of 20 photovoltaic modules, each of which consisted of a square off-axis parabolic mirror and a TaiCrystal InGaP/InGaAs/Ge TJ solar cell.<sup>[25]</sup> A BK7-glass inverted truncated pyramid (ITP) was placed at the mirror focus to homogenize the light beam and redirect it to the solar cell. Given that the mirror and the cell surface area was, respectively,  $2000$  and  $1\text{ cm}^2$ , the concentration ratio of the system was fixed at 2000. This means that when the mirror was exposed to a  $\text{DNI}$  of  $1000\text{ W m}^{-2}$ , the radiant flux received by the cell was  $200\text{ W}$ .<sup>[26,27]</sup>

To conduct our tests, one of the HCPV modules was adapted by removing the TJ solar cell and replacing it with an OF mount. The cell and the optically glued ITP were then installed indoors in a protected and isolated environment. The remaining modules were left unmodified and served as a control. On the last day of measurements, four additional modules were upgraded so that all the OFs could be simultaneously exposed to the sunlight.

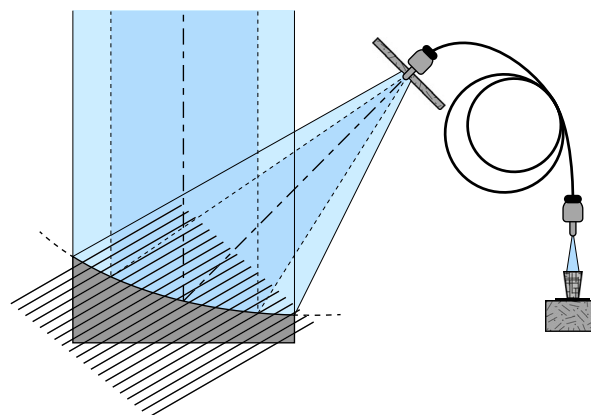


**Figure 5.** Schematic of the prototypical optical fibre-based DL/HCPV module (not in scale). The sunlight is captured by the off-axis parabolic mirror and reflected to the focus. A big portion of the light (the dark-blue beam) is injected into the optical fibre while the remaining part (the light-blue beam) is blocked by the fibre supporting structure which functions as a diaphragm. At the end of the optical path, the light is projected onto a BK7-glass inverted truncated pyramid and redirected to the solar cell.

**Optical Fibers:** Five commercial OFs were selected as representatives of different cladding/core materials and optical properties. Three of them were Thorlabs pure-silica core, hard-polymer cladding, multimode, step-index fibers with a NA of 0.50, and either a low- or high-OH content.<sup>[22]</sup> The other two were an iXBlue Photonics Ge-doped silica, single-mode OF, and an iXBlue Photonics pure-silica core, F-doped silica cladding, multimode, and step-index fiber.<sup>[28]</sup> Some relevant specifications of the selected OFs are shown in Table 1.

The experiments were conducted at the Cyprus Institute ( $35.1^\circ\text{N}$ ,  $33.4^\circ\text{E}$ ) during the second half of October under a maximum  $\text{DNI}$  of  $830 \pm 12\text{ W m}^{-2}$ . Each day, a different fiber ( $l = 2.50\text{ m}$ ) was mounted on the upgraded version of the HCPV module and its position was optimized to achieve the highest light injection. The fiber far end was fixed to a supporting structure placed indoors and coupled to the underlying solar cell. The schematic of the experimental setup and the pictures of the real module are shown in Figure 1 and 5. The photogenerated power was acquired for 8 h with a resolution of 5 min using a Fluke 87 V MAX TRMS Digital Multimeter.<sup>[29]</sup> The  $\text{DNI}$  was measured every second with a DeltaOhm LP PYRHE 16 AC Pyrheliometer<sup>[30]</sup> installed on top of the solar monitoring station (typical sensitivity:  $5\mu\text{V W}^{-1}\text{ m}^{-2}$ ). In the last measurement, all the fibers were simultaneously mounted on five different solar modules and exposed to sunlight for 10 min. The  $\text{DNI}$  and the power generated by the cells coupled to them were recorded using the same instruments as earlier.

### Acknowledgements

The authors acknowledge funding from the National Operational Programme for Research and Innovation 2014–2020, grant no. DOT1308583, and H2020 project ZeroPlus, grant agreement ID: 678407. The authors would also like to thank G. Napoli (Dipartimento di Fisica e Chimica – Emilio Segrè, Università degli Studi di Palermo) for technical assistance.

### Conflict of Interest

The authors declare no conflict of interest.

### Data Availability Statement

Research data are not shared.

## Keywords

high-concentration photovoltaics, hybrid daylighting, solarization-resistant optical fibers

Received: January 16, 2021

Revised: May 11, 2021

Published online: June 6, 2021

- 
- [1] H. Apostoleris, M. Stefancich, M. Chiesa, in *Concentrating Photovoltaics (CPV): The Path Ahead*. Springer International Publishing, Cham **2017**, pp. 1–7.
- [2] P. Pérez-Higueras, E. Muñoz, G. Almonacid, P. Vidal, *Renewable Sustainable Energy Rev.* **2011**, *15*, 1810.
- [3] D. Talavera, J. Ferrer-Rodríguez, P. Pérez-Higueras, J. Terrados, E. Fernández, *Energy Convers. Manage.* **2016**, *127*, 679.
- [4] H. Apostoleris, M. Stefancich, M. Chiesa, *Nat. Energy* **2016**, *1*, 4.
- [5] D. Chemisana, A. Zacharopoulos, in *High Concentrator Photovoltaics*, Springer International Publishing, Cham **2015**, pp. 353–376.
- [6] R. Núñez, I. Antón, G. Sala, *Light. Res. Technol.* **2017**, *50*, 1082.
- [7] R. Núñez, I. Antón, G. Sala, *Opt. Express* **2013**, *21*, 4864.
- [8] M. V. Lapsa, L. C. Maxey, D. D. Earl, D. L. Beshears, C. D. Ward, J. E. Parks, *Energy Eng.* **2007**, *104*, 7.
- [9] L. Sedki, M. Maaroufi, *Energy Build.* **2017**, *152*, 434.
- [10] I. Ullah, S. Shin, *Energy Build.* **2014**, *72*, 246.
- [11] I. Ullah, A. Whang, *Energies* **2015**, *8*, 7185.
- [12] I. Ullah, *Sol. Energy* **2020**, *196*, 484.
- [13] N.-H. Vu, S. Shin, *Sol. Energy* **2016**, *136*, 145.
- [14] T. Pham, N. Vu, S. Shin, *Buildings* **2017**, *7*, 92.
- [15] A. Aslian, B. H. S. Asli, C. J. Tan, F. R. M. Adikan, A. Toloei, *Int. J. Photoenergy* **2016**, *2016*, 1.
- [16] G. M. Lo Piccolo, A. Morana, A. Alessi, A. Boukenter, S. Girard, Y. Ouerdane, F. M. Gelardi, S. Agnello, M. Cannas, *J. Non-Cryst. Solids* **2021**, *552*, 120458.
- [17] D. L. Griscom, *Nucl. Instr. Methods Phys. Res. Sect. B* **1984**, *1*, 481.
- [18] S. Girard, A. Alessi, N. Richard, L. Martin-Samos, V. D. Michele, L. Giacomazzi, S. Agnello, D. D. Francesca, A. Morana, B. Winkler, I. Reghioua, P. Paillet, M. Cannas, T. Robin, A. Boukenter, Y. Ouerdane, *Rev. Phys.* **2019**, *4*, 100032.
- [19] A. Saha, N. Manna, *Optoelectronics and Optical Communication*, Laxmi Publications, New Delhi **2011**.
- [20] M. Cannas, F. Messina, *J. Non-Cryst. Solids* **2005**, *351*, 1780.
- [21] *Standard Tables for Reference Solar Spectral Irradiances: Direct Normal and Hemispherical on 37 Tilted Surface*, ASTM G173-03(2012), ASTM International, West Conshohocken, PA **2012**.
- [22] Thorlabs, 0.50 NA Hard Polymer-Clad Multimode Fibers, <https://www.thorlabs.com> (accessed: January 2021).
- [23] C. R. Osterwald, G. Siefer, in *Handbook of Concentrator Photovoltaic Technology*, John Wiley & Sons, Ltd, Hoboken, NJ **2016**, pp. 589–614.
- [24] E. Shittu, F. Paredes, B. Schiavo, L. Venezia, S. Milone, F. Montagnino, M. Kolokotroni, *E3S Web Conf.* **2019**, *111*, 06007.
- [25] F. Paredes, F. M. Montagnino, P. Salinari, G. Bonsignore, S. Milone, S. Agnello, M. Barbera, F. M. Gelardi, L. Sciortino, A. Collura, U. L. Cicero, M. Cannas, *AIP Conf. Proc.* **2015**, *1679*, 100003.
- [26] G. Bonsignore, A. A. Gallitto, S. Agnello, M. Barbera, R. Candia, M. Cannas, A. Collura, I. Dentici, F. M. Gelardi, U. L. Cicero, F. M. Montagnino, F. Paredes, L. Sciortino, *AIP Conf. Proc.* **2014**, *1616*, 102.
- [27] G. Bonsignore, A. A. Gallitto, S. Agnello, M. Barbera, F. M. Gelardi, L. Sciortino, A. Collura, U. L. Cicero, S. Milone, F. M. Montagnino, F. Paredes, M. Cannas, *AIP Conf. Proc.* **2015**, *1679*, 050004.
- [28] iXBlue Photonics, Custom optical fibres, <https://www.photonics.ixblue.com> (accessed: January 2021).
- [29] Fluke, 87V MAX TRMS Digital Multimeter, <https://www.fluke.com> (accessed: January 2021).
- [30] DeltaOhm, LP PYRHE 16 AC Pyrheliometer Specs sheet, <http://www.deltaohm.com> (accessed: January 2021).